MODAL IDENTITIES FOR MULTIBODY ELASTIC SPACECRAFT -- AN AID TO SELECTING MODES FOR SIMULATION

Hari B. Hablani†
Rockwell International, Seal Beach, California

ABSTRACT

This paper answers the question: Which set of modes furnishes a higher fidelity math model of dynamics of a multibody, deformable spacecraft--hinges-free or hinges-locked vehicle modes? Two sets of general, discretized, linear equations of motion of a spacecraft with an arbitrary number of deformable appendages, each articulated directly to the core body, are obtained using the above two families of modes. By a comparison of these equations, ten sets of modal identities are constructed which involve modal momenta coefficients and frequencies associated with both classes of modes. The sums of infinite series that appear in the identities are obtained in terms of mass, and first and second moments of inertia of the appendages, core body, and vehicle by using certain basic identities concerning appendage modes. Applying the above identities to a four-body spacecraft, the hinges-locked vehicle modes are found to yield a higher fidelity model than hinges-free modes, because the latter modes have nonconverging modal coefficients--a characteristic proved and illustrated in the paper.

I. INTRODUCTION

The use of appendage modes for simulating dynamics and control of multibody flexible spacecraft is widespread, in as much as they are eminently suitable for both small angle (linear) and large angle (nonlinear) dynamics. To win this benefit, however, a simulation engineer must retain a sufficient number of these modes for each appendage so that the simulation program has acceptable fidelity. When there are a large number of appendages in a spacecraft, and/or an appendage has a large mass and moment of inertia relative to those of the rigid core body of the spacecraft, the total number of appendage modes for a high accuracy model may become unacceptably great (Reference 1), possibly diminishing the utility of the appendage modes for simulation. Furthermore, control systems for a multibody spacecraft are most easily designed by considering one axis of one body at a time, because different bodies generally serve different purposes and so the control systems' intrinsic features are generally quite different. Having designed them so, to ensure they all perform as desired in the mutual presence and in the presence of flexibility, a compact mathematical model of the entire spacecraft's dynamics is desired so that the control designs can be refined fast and economically about all axes. For this purpose, the linear, small angle models of spacecraft flexible dynamics are just right, and so the engineer could beneficially employ the vehicle modes of the spacecraft. Hughes[2] conceived of two families of vehicle modes for multibody spacecraft: "hinges-free" and "hinges-locked" vehicle modes (although he does not use this terminology). By definition, hinges-free modes are obtained by leaving all hinges free, that is, unlocked and unforced, so that the associated natural vehicle modes may contain motion of the articulated bodies relative to the inboard bodies. Conversely, in the hinges-locked modes, the relative motion of the articulated bodies is, by definition, zero, and some force or torque is applied at the hinges to keep the motion so. In Reference 3, these vehicle modes are formulated, and their zero linear and angular momentum properties, the orthogonality conditions, and the associated modal momenta coefficients are theorized.

A critical question whose answer is sought in this paper is: Between the hinges-free and hinges-locked vehicle modes, which one furnishes a higher fidelity dynamic model, retaining the same number of modes in the simulation? To this end, a multibody spacecraft is considered in this paper that consists of a rigid core body, and N flexible appendages, each articulated directly to the core body. Three sets of discrete motion equations of this spacecraft are obtained from a continuum set by using appendage modes, hinges-free vehicle modes, and hinges-locked vehicle modes. To compare the last two families of modes, modal identities are devised that express the sum of contribution of all infinite number of modes in terms of first and second moments of inertia of the articulated bodies, the core body, and the vehicle, following Hughes[4]. The analysis is amply illustrated, and definitive conclusions are summarized at the end of the paper. Although for concreteness, the paper considers a multibody spacecraft with level-1 articulated bodies (the terminology of Ho[5]), it will be clear that the conclusions drawn apply to a wider range of multibody spacecraft.

II. FORMULATION OF CONTINUUM EQUATIONS OF MOTION

Fig. 1 portrays an N+1-body spacecraft that consists of a three-axis stabilized core rigid body B_0, and deformable bodies $E_1,\ldots,E_N$, each articulated directly to the core body. The motion equations will be developed with respect to the

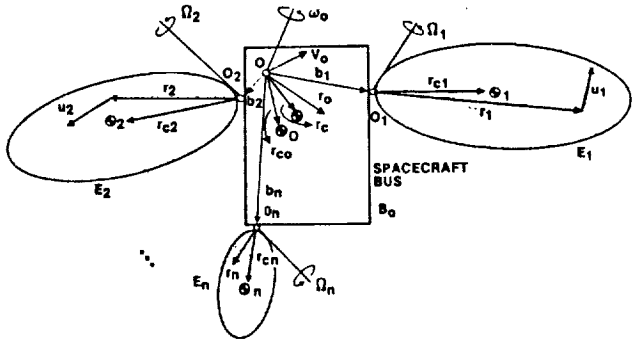

Figure 1. An N+1-Body Spacecraft With N Articulated, Deformable Appendages

†Engineering Specialist, Guidance and Control Group, AIAA Senior Member.

reference point 0 in Fig. 1 which is neither the mass center $\oplus_0$ of the body B_0, nor the mass center $\oplus$ of the entire vehicle V. This generality in the formulation is warranted because the NASTRAN modal data corresponding to such multibody spacecraft are often with respect to an arbitrary reference node 0, and the mass centers are generally nodeless empty points. The mass of each body is denoted m_p (p=0,1,...,N); the mass of all N articulated bodies together, m_e; and the mass of entire spacecraft, m; clearly, $m = m_0 + m_e$. The first moment of mass of B_0 relative to 0 is $\underline{c}_0$, and those for the hinged bodies (j=1,...,N), measured from the respective hinges O_j, are denoted $\underline{c}_j$. Similar to $\underline{c}_p$ (p=0,1,...,N), the vector $\underline{r}_0$ emanates from 0 and $\underline{r}_j$ from O_j. Note that the subscript p covers all bodies, while j covers only the articulated bodies. The vectors $\underline{b}_j$ (j=1,...,N) originating from 0 locate the hinges O_j of the hinged bodies E_j. The first moment of inertia of the entire spacecraft, then, is

$$\underline{c} = \underline{c}_0 + \sum_j (m_j \underline{b}_j + \underline{C}_{0j}\underline{c}_j) \triangleq \underline{c}_0 + \underline{c}_e; \quad \sum_j = \sum_{j=1}^{N} \qquad (1)$$

where the matrix $\underline{C}_{0j}$ transforms the E_j-fixed vector $\underline{c}_j$ to a B_0-fixed vector, and the vectors $\underline{b}_j$ are expressed in the B_0-fixed frame. Next, $\underline{J}_0$ denotes the inertia matrix of the body B_0 about the reference point 0, while $\underline{J}_j$ is the inertia matrix of the hinged body E_j in its own frame about the hinge O_j. The inertia matrix of E_j expressed at the reference point 0 in the B_0-fixed frame is denoted $\underline{J}_j^0$ and

$$\underline{J}_j^0 = \underline{C}_{0j}\,\underline{J}_j\,\underline{C}_{j0} - [m_j \underline{b}_j^x\,\underline{b}_j^x + \underline{b}_j^x\,(\underline{C}_{0j}\,\underline{c}_j)^x + (\underline{C}_{0j}\,\underline{c}_j)^x \underline{b}_j^x] \qquad (2)$$

where $(\bullet)^x$ means the 3x3 skew-symmetrix matrix associated with the vector $(\bullet)$. The inertia matrix $\underline{J}$ of the entire vehicle at the point 0 will then be

$$\underline{J} = \underline{J}_0 + \sum_j \underline{J}_j^0 \triangleq \underline{J}_0 + \underline{J}_e^0 \qquad (3)$$

Anticipating our later needs, the cross inertia matrix $\underline{J}_{0j}$ between the bodies B_0 and E_j expressed in the E_j-fixed frame equals

$$\underline{J}_{0j} \triangleq \underline{J}_j - (\underline{C}_{j0}\underline{b}_j)^x\,\underline{c}_j^x \qquad (4)$$

As for the motion of the spacecraft, its mass center is assumed to perform some orbital motion, not coupled with its attitude motion under consideration. To develop motion equations, the local orbital frame is taken to be an inertial frame. The kinetic quantities of interest are: $\underline{V}_0(t)$, the perturbational velocity of the reference point 0 over the uniform orbital motion at time t; $\omega_0(t)$, the inertial angular velocity of B_0; $\underline{\Omega}_j(t)$, the angular velocity of each articulated body E_j relative to B_0 at the hinge O_j; and $\underline{u}_j(\underline{r}_j,t)$, the deformation of E_j at the location $\underline{r}_j \in E_j$. These quantities are taken to be linear, first order, infinitesimal, so that their products can be ignored in the analysis. The external forces and torques acting on the spacecraft are the force $\underline{f}_0(t)$ and the torque $\underline{g}_0(t)$ acting on B_0 at 0, and the force $\underline{f}_j(t)$ and the torque $\underline{g}_j(t)$ on each E_j at the hinge O_j. The latter pair, $(\underline{f}_j,\underline{g}_j)$, includes a distributed force $\underline{\beta}_j(\underline{r}_j,t)$ acting in the domain of the body E_j, and if $\underline{\beta}_j(\underline{r}_j,t)$ is the only surface force acting on E_j, then

$$\underline{f}_j(t) = \int_j \underline{\beta}_j(\underline{r}_j,t)\,dA$$
$$\underline{g}_j(t) = \int_j \underline{r}_j^x \underline{\beta}_j(\underline{r}_j,t)\,dA \qquad (5)$$

where dA is an elemental area of E_j and $\int_j \triangleq \int_{E_j}$. With the aid of the Dirac delta function and its derivative, the distributed force $\underline{\beta}_j(\underline{r}_j,t)$ also represents a distributed moment. Regarding the control forces and torques, those acting on B_0 are included in the quantities $\underline{f}_0$ and $\underline{g}_0$, whereas, if a control force or torque is produced in the interior domain of E_j without acting against the core body B_0, then that is included in the pair $(\underline{f}_j,\underline{g}_j)$; however, if, for instance, the torque is produced by an electric motor which rests on B_0 at the interface O_j and exerts on E_j, then this is considered separately and denoted $\underline{g}_{0j}(t)$ (j=1,...,N), for it produces a reaction torque $-\underline{g}_{0j}(t)$ which acts on B_0. The total force $\underline{f}(t)$ and torque $\underline{g}(t)$ that act on the vehicle are

$$\underline{f} = \underline{f}_0 + \sum_j \underline{C}_{0j}\underline{f}_j, \quad \underline{g} = \underline{g}_0 + \sum_j (\underline{C}_{0j}\underline{g}_j + \underline{b}_j^x \underline{C}_{0j}\underline{f}_j) \qquad (6)$$

where, of course, $\underline{g}(t)$ does not include the control torque $\underline{g}_{0j}(t)$ at the interface O_j.

The elastic spacecraft under consideration is relatively simple; it is straightforward to develop its linear, continuum motion equations following Hughes[4,6,7]. The equations governing the discrete variables $\underline{V}_0, \underline{\omega}_0, \underline{\Omega}_j$ (j=1,...,N) are:

$$m\dot{\underline{V}}_0 - \underline{c}^x\dot{\underline{\omega}}_0 - \sum_j \underline{C}_{0j}\underline{c}_j^x\ddot{\underline{\Omega}}_j + \sum_j \int_j \underline{C}_{0j}\ddot{\underline{u}}_j\,dm = \underline{f}$$

$$\underline{c}^x\dot{\underline{V}}_0 + \underline{J}\,\dot{\underline{\omega}}_0 + \sum_j \underline{C}_{0j}\underline{J}_{0j}\ddot{\underline{\Omega}}_j + \sum_j \int_j (\underline{b}_j^x\underline{C}_{0j} + \underline{C}_{0j}\underline{r}_j^x)\,\ddot{\underline{u}}_j\,dm = \underline{g} \qquad (7)$$

$$\underline{c}_j^x\underline{C}_{j0}\dot{\underline{V}}_0 + (\underline{C}_{0j}\underline{J}_{0j})^T\dot{\underline{\omega}}_0 + \underline{J}_j\dot{\underline{\Omega}}_j + \int_j \underline{r}_j^x\ddot{\underline{u}}_j\,dm = \underline{g}_{0j} + \underline{g}_j \quad (j = 1,...,N)$$

where an overdot indicates differentiation with respect to time. To write the motion equation governing the deformation $\underline{u}_j(\underline{r}_j,t)$ of the flexible body E_j, denote the related linear stiffness operator by $\underline{L}_j$; the body E_j is allowed to be anisotropic and/or nonhomogeneous, and its mass

density is denoted $\sigma_j(\underline{r}_j)$. The continuum motion equation governing the deformation $\underline{u}_j$ is then:

$$\underline{L}_j\underline{u}_j + \sigma_j \{\underline{C}_{j0}\dot{\underline{V}}_0 - (\underline{C}_{j0}\underline{b}_j + \underline{r}_j)^x \underline{C}_{j0}\dot{\underline{\omega}}_0 - \underline{r}_j^x\dot{\underline{\Omega}}_j + \ddot{\underline{u}}_j\} = \underline{\phi}_j(\underline{r}_j,t) \quad (j=1,\ldots,N) \tag{8}$$

The continuum motion equations (7) and (8) are discretized in the next section.

III. DISCRETIZATION OF CONTINUUM EQUATIONS OF MOTION

Three families of modes will be employed in this section for discretization: (1) appendage modes, (2) hinges-free vehicle modes, and (3) hinges-locked vehicle modes. The use of appendage modes is standard; they are employed here in order to evaluate the infinite sums that appear in the hinges-free and hinges-locked modal identities in Section IV in terms of mass, and first and second moments of inertia of the appendages, core body, and the vehicle.

DISCRETIZATION BY APPENDAGE MODES

Following Hughes[4], define the modal momenta coefficients $\underline{P}_{j\sigma}$ and $\underline{H}_{j\sigma}$ concerning the appendage (cantilever) modes $\underline{U}^a_{j\sigma}(\underline{r}_j)$ of the articulated body E_j:

$$\underline{P}_{j\sigma} \triangleq \int_j \underline{U}^a_{j\sigma}(\underline{r}_j)\, dm \quad (j=1,\ldots,N;\sigma=1,\ldots,\infty)$$

$$\underline{H}_{j\sigma} \triangleq \int_j \underline{r}_j^x \underline{U}^a_{j\sigma}(\underline{r}_j)\, dm \tag{9}$$

where dm = elemental mass. The coefficient $\underline{P}_{j\sigma}$ is associated with linear momentum and $\underline{H}_{j\sigma}$ with angular momentum of the mode σ at the hinge point O_j. The modal angular momentum coefficient relative to the reference point O (Fig. 1) is defined as

$$\underline{H}^0_{j\sigma} \triangleq \underline{b}_j^x \underline{C}_{0j}\underline{P}_{j\sigma} + \underline{C}_{0j}\underline{H}_{j\sigma} \tag{10}$$

Then the continuum equations (7) and (8) discretize to

$$\begin{aligned}
&m\dot{\underline{V}}_0 - \underline{c}^x\dot{\underline{\omega}}_0 - \sum_j \underline{C}_{0j}\underline{c}_j^x\dot{\underline{\Omega}}_j + \sum_j \underline{C}_{0j}\sum_\sigma \underline{P}_{j\sigma}\ddot{Q}_{j\sigma} = \underline{f}\\
&\underline{c}^x\dot{\underline{V}}_0 + \underline{J}\,\dot{\underline{\omega}}_0 + \sum_j \underline{C}_{0j}\underline{J}_{0j}\dot{\underline{\Omega}}_j + \sum_j\sum_\sigma \underline{H}^0_{j\sigma}\ddot{Q}_{j\sigma} = \underline{g}\\
&\underline{c}_j^x\underline{C}_{j0}\dot{\underline{V}}_0 + \underline{J}^T_{0j}\underline{C}_{j0}\dot{\underline{\omega}}_0 + \underline{J}_j\dot{\underline{\Omega}}_j + \sum_\sigma \underline{H}_{j\sigma}\ddot{Q}_{j\sigma} = \underline{g}_j + \underline{g}_{0j}\\
&\underline{P}^T_{j\sigma}\underline{C}_{j0}\dot{\underline{V}}_0 + \underline{H}^{0T}_{j\sigma}\dot{\underline{\omega}}_0 + \underline{H}^T_{j\sigma}\dot{\underline{\Omega}}_j + \ddot{Q}_{j\sigma} + \Omega^{c2}_{j\sigma}Q_{j\sigma} = \Upsilon^a_{j\sigma}\\
&\qquad (j=1,\ldots,N;\ \sigma=1,\ldots,\infty)
\end{aligned} \tag{11}$$

where the superscript T indicates transpose of the quantity; $Q_{j\sigma}(t)$ is the modal coordinate and $\Omega^c_{j\sigma}$ is the frequency associated with the σ-th appendage mode $\underline{U}^a_{j\sigma}(\underline{r}_j)$ of the body E_j; and $\Upsilon^a_{j\sigma}(t)$ is the modal input to that mode:

$$\Upsilon^a_{j\sigma}(t) = \int_j \underline{U}^{aT}_{j\sigma}(\underline{r}_j)\underline{\phi}_j(\underline{r}_j,t)\, dA \tag{12}$$

Eqs. (11) are a generalization of Eq. (35) of Hughes[4], for the former include articulation motion of the appendages. Much more complex and general equations than Eqs. (11) are available in the vast literature on deformable multibody dynamics; see, for instance, the works of Ho[5], and Singh et al[8] on spacecraft with arbitrary tree topology. Eqs. (11) nevertheless may boast of simplicity which is eminently useful while designing the control systems for articulated bodies. More importantly though, Eqs. (11) are derived here because in Section IV they will aid in developing modal identities. To facilitate this task, Eqs. (11) are abbreviated by using the definitions

$$\begin{aligned}
&\underline{C}_A^{0T} \triangleq -[\underline{C}_{01}\underline{c}_1^x, \ldots, \underline{C}_{0N}\underline{c}_N^x],\\
&\underline{J}^T_{0A} \triangleq [\underline{C}_{01}\underline{J}_{01}, \ldots, \underline{C}_{0N}\underline{J}_{0N}]\\
&\underline{P}_j^T \triangleq [\underline{P}_{j1}\ \ \underline{P}_{j2}\ \ldots],\\
&\underline{P}_A^{0T} \triangleq [\underline{C}_{01}\underline{P}_1^T, \ldots, \underline{C}_{0N}\underline{P}_N^T]\\
&\underline{H}_j^{0T} \triangleq [\underline{H}^0_{j1}\ \ \underline{H}^0_{j2}\ \ldots],\\
&\underline{H}_A{}^{0T} \triangleq [\underline{H}_1^{0T}, \ldots, \underline{H}_N^{0T}]\\
&\underline{H}_j^T \triangleq [\underline{H}_{j1}\ \ \underline{H}_{j2}\ \ldots],\\
&\underline{H}_A \triangleq \text{diag}\,[\underline{H}_1 \ldots \underline{H}_N],\ \underline{J}_A \triangleq \text{diag}\,[\underline{J}_1 \ldots \underline{J}_N]\\
&\underline{Q}_j^T \triangleq [Q_{j1}\ Q_{j2}\ \ldots], \qquad \underline{Q}_A^T \triangleq [\underline{Q}_1^T \ldots \underline{Q}_N^T],\\
&\underline{g}_A^T \triangleq [\underline{g}_1^T \ldots \underline{g}_N^T],\\
&\underline{g}^T_{0A} \triangleq [\underline{g}^T_{01} \ldots \underline{g}^T_{0N}], \quad \underline{\Omega}_A^T \triangleq [\underline{\Omega}_1^T \ldots \underline{\Omega}_N^T]\\
&\underline{\Omega}_j^c \triangleq \text{diag}\,[\Omega^c_{j1}\ \Omega^c_{j2}\ldots], \qquad \underline{\Omega}_c \triangleq \text{diag}\,[\underline{\Omega}_1^c \ldots \underline{\Omega}_N^c]\\
&\underline{\Upsilon}_j^{aT} \triangleq [\Upsilon^a_{j1}\ \ \Upsilon^a_{j2}\ \ldots], \qquad \underline{\Upsilon}_A^{aT} \triangleq [\underline{\Upsilon}_1^{aT} \ldots \underline{\Upsilon}_N^{aT}]
\end{aligned} \tag{13}$$

Eqs. (11) then take this concise form:

$$\begin{aligned}
&m\dot{\underline{V}}_0 - \underline{c}^x\dot{\underline{\omega}}_0 + \underline{C}_A^{0T}\dot{\underline{\Omega}}_A + \underline{P}_A^{0T}\ddot{\underline{Q}}_A = \underline{f}\\
&\underline{c}^x\dot{\underline{V}}_0 + \underline{J}\,\dot{\underline{\omega}}_0 + \underline{J}^T_{0A}\dot{\underline{\Omega}}_A + \underline{H}_A^{0T}\ddot{\underline{Q}}_A = \underline{g}\\
&\underline{C}_A^{0}\dot{\underline{V}}_0 + \underline{J}_{0A}\dot{\underline{\omega}}_0 + \underline{J}_A\dot{\underline{\Omega}}_A + \underline{H}_A^T\ddot{\underline{Q}}_A = \underline{g}_A + \underline{g}_{0A}\\
&\underline{P}_A^{0}\dot{\underline{V}}_0 + \underline{H}_A^{0}\dot{\underline{\omega}}_0 + \underline{H}_A\dot{\underline{\Omega}}_A + \ddot{\underline{Q}}_A + \underline{\Omega}_c^2\underline{Q}_A = \underline{\Upsilon}_A^a
\end{aligned} \tag{14}$$

It is interesting to compare Eqs. (14) with Eqs. (43) of Hughes[4]. For even more compaction of these equations, the following matrices are introduced:

$$\underline{M}_{VV} \triangleq \begin{bmatrix} m\underline{1} & -\underline{c}^{\times} \\ \underline{c}^{\times} & \underline{J} \end{bmatrix}, \quad \underline{M}_{VA} \triangleq [\underline{C}_A^0 \quad \underline{J}_{0A}], \quad \overset{\bullet\bullet}{\underline{q}}_V^T \triangleq [\underline{v}_0^T \quad \underline{\omega}_0^T]$$

$$\underline{\mathcal{P}}_A^0 \triangleq [\underline{P}_A^0 \quad \underline{H}_A^0], \quad \underline{u}_V^T \triangleq [\underline{f}^T \quad \underline{g}^T] \tag{15}$$

where $\underline{1}$ is a 3x3 identity matrix. Eqs. (14) thereby reduce to the following three matrix equations: one governing six overall degrees of freedom of the spacecraft, $\underline{q}_V(t)$; the second governing n_a x1 vector $\underline{\Omega}_A$ of n_a relative angular velocities of N articulated bodies; and the third governing the ∞x1 vector $\underline{Q}_A$ of modal coordinates of appendage modes of all articulated bodies.

$$\underline{M}_{VV}\overset{\bullet\bullet}{\underline{q}}_V + \underline{M}_{VA}^T\dot{\underline{\Omega}}_A + \underline{\mathcal{P}}_A^{0\,T}\overset{\bullet\bullet}{\underline{Q}}_A = \underline{u}_V(t) \tag{16.a}$$

$$\underline{M}_{VA}\overset{\bullet\bullet}{\underline{q}}_V + \underline{J}_A\dot{\underline{\Omega}}_A + \underline{H}_A^T\overset{\bullet\bullet}{\underline{Q}}_A = \underline{g}_A(t) + \underline{g}_{0A}(t) \tag{16.b}$$

$$\underline{\mathcal{P}}_A^0\overset{\bullet\bullet}{\underline{q}}_V + \underline{H}_A\dot{\underline{\Omega}}_A + \overset{\bullet\bullet}{\underline{Q}}_A + \underline{\Omega}_c^2\underline{Q}_A = \underline{Y}_A^a(t) \tag{16.c}$$

Modal identities associated with the modal momenta matrices $\underline{\mathcal{P}}_A^0$ and $\underline{H}_A$ are derived in Section IV.

DISCRETIZATION BY HINGES-FREE VEHICLE MODES

In this technique, the continuum equations (7) and (8) are discretized all at once. For this purpose, the following modal expansion is postulated for the variables in Eqs. (7) and Eq. (8) (Reference 3):

$$\begin{aligned}
\underline{v}_0(t) &= \dot{\underline{R}}_0(t) + \Sigma\, \underline{\chi}_{0\nu}\dot{\eta}_\nu(t), \\
\underline{\omega}_0(t) &= \dot{\underline{\Theta}}_0(t) + \Sigma\, \underline{\phi}_{0\nu}\dot{\eta}_\nu(t), \\
\underline{\Omega}_j(t) &= \dot{\underline{\Theta}}_j(t) + \textstyle\sum \underline{\phi}_{j\nu}\dot{\eta}_\nu(t), \\
\underline{u}_j(\underline{r}_j,t) &= \textstyle\sum \underline{U}_{j\nu}(\underline{r}_j)\eta_\nu(t), \quad \sum = \sum_{\nu=1}^{\infty}, \\
&\qquad (j=1,2,\ldots,N)
\end{aligned} \tag{17}$$

where $\underline{R}_0$, $\underline{\Theta}_0$, and $\underline{\Theta}_j$ are the temporal coordinates for the rigid modes of the spacecraft; the total number of articulation degrees of freedom is n_a, so there are n_a+6 rigid modes in all. Furthermore, $\underline{R}_0$ is the translation of the reference point 0, and $\underline{\Theta}_0$ is the rotation of the spacecraft, both in rigid modes; similarly, $\underline{\Theta}_j$ is the rotation of the hinged body E_j relative to B_0 at the hinge 0_j (j=1,...,N) in a rigid mode. The quantities $\underline{\chi}_{0\nu}$, $\underline{\phi}_{0\nu}$, and $\underline{\phi}_{j\nu}$ (j=1,...,N; ν=1,...,∞) are ν-th modal coefficients contributing, respectively, to overall discrete motions $\underline{v}_0$, $\underline{\omega}_0$, and $\underline{\Omega}_j$; and $\eta_\nu(t)$ is the associated modal coordinate. The eigenfunction $\underline{U}_{j\nu}(\underline{r}_j)$ is that part of the hinges-free vehicle mode, denoted $\underline{W}_\nu(\underline{r})$, which defines the deformation of body E_j in ν-th mode. Although $\underline{U}_{j\nu}(\underline{r}_j)$ satisfies the condition of zero displacement and zero rotation at the hinge 0_j, that is, $\underline{U}_{j\nu}(0_j) = \underline{0}$ and $\frac{1}{2}\nabla^{\times}\underline{U}_{j\nu}(0_j) = \underline{0}$, it is not the same as the σ-th appendage mode $\underline{U}_{j\sigma}^a(\underline{r}_j)$ used before, because in the case of $\underline{U}_{j\nu}(\underline{r}_j)$, no torque acts, by definition, at the hinge 0_j to enforce the zero deformation and zero rotation condition, whereas in the case of $\underline{U}_{j\sigma}^a(\underline{r}_j)$, the immobile support of the appendage enforces that condition. Because of the mobile support of the hinge 0_j, the total motion $\underline{W}_{j\nu}(\underline{r}_j)$ of E_j in an inertial frame is

$$\underline{W}_{j\nu}(\underline{r}_j) = \underline{\chi}_{0\nu} - (\underline{b}_j + \underline{C}_{0j}\underline{r}_j)^{\times}\underline{\phi}_{0\nu} - \underline{C}_{0j}\underline{r}_j^{\times}\underline{\phi}_{j\nu} + \underline{C}_{0j}\underline{U}_{j\nu}(\underline{r}_j) \quad (j=1,\ldots,N;\ \nu=1,\ldots,\infty) \tag{18}$$

where the first two terms in the right side are because of the translation and rotation of the core body in the ν-th mode, and the third term $\underline{r}_j^{\times}\underline{\phi}_{j\nu}$ is caused by the relative rotation of E_j at the free hinge 0_j. The motion of the core body in ν-th mode is given simply by

$$\underline{W}_{0\nu}(\underline{r}_0) = \underline{\chi}_{0\nu} - \underline{r}_0^{\times}\underline{\phi}_{0\nu} \tag{19}$$

Thus a hinges-free vehicle mode $\underline{W}_\nu(\underline{r})$spans entire spacecraft such that

$$\underline{W}_\nu(\underline{r}) = \begin{cases} \underline{W}_{0\nu}(\underline{r}_0), & \text{if } \underline{r} = \underline{r}_0 \\ \underline{W}_{j\nu}(\underline{r}_j), & \text{if } \underline{r} = \underline{b}_j + \underline{C}_{0j}\underline{r}_j \end{cases} \quad (j=1,\ldots,N;\ \nu=1,\ldots,\infty) \tag{20}$$

Following Hughes[2], the $6+n_a$ rigid modes of a spacecraft with articulated bodies are $\underline{1}$, $-\underline{r}^{\times}$, and $-\underline{r}_j^{\times}$ (j=1,...,n_a). Not surprisingly, the elastic modes $\underline{W}_\nu^a(\underline{r})$ (ν=1,...,∞) are orthogonal to these rigid modes; that is:

$$\int_V \underline{W}_\nu(\underline{r})\,dm = \underline{0}, \quad \int_V \underline{r}^{\times}\underline{W}_\nu(\underline{r})\,dm = \underline{0},$$

$$\int_j \underline{r}_j^{\times}\underline{W}_{j\nu}(\underline{r}_j)\,dm = \underline{0} \tag{21.a,b,c}$$

where $\int_V$ means the entire vehicle is the domain of integration. Eqs. (21) can be verified by substituting the expansion (17) in the continuum equations (7) with zero right sides. Indeed, Eqs. (21a,b) state that the linear and angular momentum residing in a ν-th hinges-free vehicle mode are zero, whereas Eq. (21c) expresses a zero momentum-like property of the articulated body E_j. These properties can be stated alternately by defining modal momenta coefficients $(\underline{p}_{j\nu}, \underline{h}_{j\nu})$ for each articulated body and $(\underline{p}_\nu, \underline{h}_\nu^0)$ for all articulated bodies collectively:

$$\underline{p}_{j\nu} \triangleq \int_j \underline{U}_{j\nu}(\underline{r}_j)\,dm \qquad \underline{h}_{j\nu} \triangleq \int_j \underline{r}_j^{\times}\underline{U}_{j\nu}(\underline{r}_j)\,dm$$

$$\underline{p}_\nu \triangleq \sum_j \underline{C}_{0j}\underline{p}_{j\nu} \qquad \underline{h}_\nu^0 = \sum_j \left[\underline{b}_j^{\times}\underline{C}_{0j}\underline{p}_{j\nu} + \underline{C}_{0j}\underline{h}_{j\nu}\right] \tag{22}$$

where $\underline{h}_\nu^0$ is defined relative to the reference point 0. These may be compared with the definitions (9) and (10). The zero momentum

properties (21) then transform to:

$$m\,\underline{\chi}_{0\nu} - \underline{c}^{\times}\underline{\phi}_{0\nu} - \sum_j \underline{C}_{0j}\underline{c}_j^{\times}\underline{\phi}_{j\nu} + \underline{p}_\nu = \underline{0}$$

$$\underline{c}^{\times}\underline{\chi}_{0\nu} + \underline{J}\,\underline{\phi}_{0\nu} + \sum_j \underline{C}_{0j}\underline{J}_{0j}\underline{\phi}_{j\nu} + \underline{h}_\nu^0 = \underline{0}$$

$$\underline{c}_j^{\times}\,\underline{C}_{j0}\underline{\chi}_{0\nu} + \underline{J}_{0j}^T\underline{C}_{j0}\underline{\phi}_{0\nu} + \underline{J}_j\underline{\phi}_{j\nu} + \underline{h}_{j\nu} = \underline{0}$$

$$(j=1,\ldots N;\ \nu=1,\ldots,\infty) \qquad (23)$$

The eigenvalue problem which governs a hinges-free vehicle mode is given by

$$\underline{L}_j\underline{U}_{j\nu}(\underline{r}_j) = \sigma_j\omega_\nu^2\underline{C}_{j0}\underline{W}_{j\nu}(\underline{r}_j) \quad (j=1,\ldots,N;\ \nu=1,\ldots,\infty) \qquad (24)$$

where ω_ν is the frequency of ν-th mode. The orthogonality conditions are obtained by performing the operation $\sum_j \int_j \underline{U}_{j\mu}^T(\underline{r}_j)\,(\bullet)\,dv$ over the eigenvalue problem (24) and recalling the properties (23). Here, dv is an elemental volume. One then obtains

$$\int_V \underline{W}_\mu^T(\underline{r})\underline{W}_\nu(\underline{r})\,dm = \delta_{\mu\nu} \qquad (25.a)$$

$$\sum_j \left\{ \int_j \underline{U}_{j\mu}^T\underline{U}_{j\nu}\,dm + \underline{h}_{j\mu}^T\underline{\phi}_{j\nu} \right\} + \underline{p}_\mu^T\underline{\chi}_{0\nu} + \underline{h}_\mu^{0T}\underline{\phi}_{0\nu} = \delta_{\mu\nu} \qquad (25.b)$$

$$\sum_j \Big[\int_j \underline{U}_{j\mu}^T\underline{U}_{j\nu}\,dm + \{\underline{\chi}_{0\mu}^T\underline{C}_{0j}\underline{c}_j^{\times}\underline{\phi}_{j\nu} - \underline{\phi}_{j\mu}^T\underline{c}_j^{\times}\underline{C}_{j0}\underline{\chi}_{0\nu}\} -$$

$$(\underline{\phi}_{j\mu}^T\underline{J}_j\underline{\phi}_{j\nu} + \underline{\phi}_{j\mu}^T\underline{C}_{j0}\underline{J}_{j0}\underline{\phi}_{0\nu} + \underline{\phi}_{0\mu}^T\underline{J}_{j0}\underline{C}_{0j}\underline{\phi}_{j\nu})\Big]$$

$$- \left[m\,\underline{\chi}_{0\mu}^T\underline{\chi}_{0\nu} + \underline{\phi}_{0\mu}^T\underline{c}^{\times}\underline{\chi}_{0\nu} - \underline{\chi}_{0\mu}^T\underline{c}^{\times}\underline{\phi}_{0\nu} + \underline{\phi}_{0\mu}^T\underline{J}\,\underline{\phi}_{0\nu}\right] = \delta_{\mu\nu} \qquad (25.c)$$

$$\sum_j \int_j \underline{U}_{j\mu}^T\,\underline{L}_j\underline{U}_{j\nu}(\underline{r}_j)\,dv = \omega_\nu^2\delta_{\mu\nu} \qquad (25.d)$$

where $\delta_{\mu\nu}$ is the Kronecker delta.

Utilizing the modal expansion (17), the zero momentum modal properties (21) and (23), and the orthogonality properties (25), the continuum equations are discretized to these decoupled equations which separately govern the rigid and elastic modes of the spacecraft:

$$m\,\ddot{\underline{R}}_0 - \underline{c}^{\times}\ddot{\underline{\Theta}}_0 - \sum_j \underline{C}_{0j}\underline{c}_j^{\times}\ddot{\underline{\Theta}}_j = \underline{f} \qquad (26.a)$$

$$\underline{c}^{\times}\ddot{\underline{R}}_0 + \underline{J}\,\ddot{\underline{\Theta}}_0 + \sum_j \underline{C}_{0j}\underline{J}_{0j}\ddot{\underline{\Theta}}_j = \underline{g} \qquad (26.b)$$

$$\underline{c}_j^{\times}\underline{C}_{j0}\ddot{\underline{R}}_0 + \underline{J}_{0j}^T\underline{C}_{j0}\ddot{\underline{\Theta}}_0 + \underline{J}_j\ddot{\underline{\Theta}}_j = \underline{g}_{0j} + \underline{g}_j \quad (j=1,\ldots,N) \qquad (26.c)$$

$$\ddot{\eta}_\nu + \omega_\nu^2\eta_\nu = \underline{\chi}_{0\nu}^T\underline{f} + \underline{\phi}_{0\nu}^T\underline{g} + \sum_j \underline{\phi}_{j\nu}^T(\underline{g}_{0j} + \underline{g}_j) + \gamma_\nu(t)$$

$$(\nu=1,2,\ldots,\infty) \qquad (26.d)$$

where $\gamma_\nu(t)$ is the scalar input to ν-th mode considering all articulated bodies collectively:

$$\gamma_\nu(t) \triangleq \sum_j \int_j \underline{U}_{j\nu}^T(\underline{r}_j)\underline{b}_j(\underline{r}_j,t)\,dA \qquad (27)$$

These equations are abbreviated by recalling appropriate definitions from (13) and (15) and by the following additional definitions

$$\underline{q}_{VR} \triangleq \begin{bmatrix}\underline{R}_0\\ \underline{\Theta}_0\end{bmatrix},\ \underline{\Theta}_A \triangleq \begin{bmatrix}\underline{\Theta}_1\\ \vdots\\ \underline{\Theta}_N\end{bmatrix},\ \underline{\chi}_0 \triangleq \begin{bmatrix}\underline{\chi}_{01}^T\\ \underline{\chi}_{02}^T\\ \vdots\end{bmatrix},\ \underline{\phi}_0 \triangleq \begin{bmatrix}\underline{\phi}_{01}^T\\ \underline{\phi}_{02}^T\\ \vdots\end{bmatrix},$$

$$\underline{\phi}_A \triangleq \begin{bmatrix}\underline{\phi}_{11}^T & \cdots & \underline{\phi}_{N1}^T\\ \underline{\phi}_{12}^T & \cdots & \underline{\phi}_{N2}^T\\ \vdots & & \vdots\end{bmatrix} \qquad \begin{aligned}\underline{\eta}_e^T &\triangleq [\eta_1\ \eta_2\ldots],\\ \underline{\omega} &= \mathrm{diag}\,[\omega_1\ \omega_2\ldots],\\ \underline{\gamma}^T &\triangleq [\gamma_1\ \gamma_2\ldots]\end{aligned} \qquad (28)$$

Here $\underline{q}_{VR}$ is a rigid mode vector, whereas $\underline{q}_V$ in (15) is a vector of overall motion of the spacecraft; the vector $\underline{\Theta}_A$ from (28) and $\underline{\Omega}_A$ in (13) differ likewise. Eqs. (26) now condense to this desired compact form:

$$\underline{M}_{VV}\ddot{\underline{q}}_{VR} + \underline{M}_{VA}^T\ddot{\underline{\Theta}}_A = \underline{u}_V$$

$$\underline{M}_{VA}\ddot{\underline{q}}_{VR} + \underline{J}_A\ddot{\underline{\Theta}}_A = \underline{g}_A + \underline{g}_{0A}$$

$$\ddot{\underline{\eta}}_e + \underline{\omega}^2\underline{\eta}_e = \underline{\chi}_0\underline{f} + \underline{\phi}_0\underline{g} + \underline{\phi}_A(\underline{g}_{0A} + \underline{g}_A) + \underline{\gamma} \qquad (29)$$

DISCRETIZATION BY HINGES-LOCKED VEHICLE MODES

Since these modes are defined by forcing the articulation motion $\underline{\Omega}_j$ (j=1,...,N) to be zero, they are obtained by a modal analysis of the first two equations in (7) and Eq. (8) from which the $\underline{\Omega}_j$ (j=1,...,N) terms are ignored. The torque actually required to keep the hinges locked can be evaluated from the third equation in (7) but that is not relevant here. The equations for the modal analysis are therefore:

$$m\dot{\underline{V}}_0 - \underline{c}^{\times}\dot{\underline{\omega}}_0 + \sum_j \int_j \underline{C}_{0j}\ddot{\underline{u}}_j\,dm = \underline{0}$$

$$\underline{c}^{\times}\dot{\underline{V}}_0 + \underline{J}\,\dot{\underline{\omega}}_0 + \sum_j \int_j (\underline{b}_j^{\times}\underline{C}_{0j} + \underline{C}_{0j}\underline{r}_j^{\times})\ddot{\underline{u}}_j\,dm = \underline{0}$$

$$\underline{L}_j\underline{u}_j + \sigma_j\{\underline{C}_{j0}\dot{\underline{V}}_0 - (\underline{C}_{j0}\underline{b}_j + \underline{r}_j)^{\times}\underline{C}_{j0}\dot{\underline{\omega}}_0 + \ddot{\underline{u}}_j\} = \underline{0} \qquad (30)$$

Eqs. (30), in fact, govern the motion of a free spacecraft with cantilevered appendages, so the sought hinges-locked vehicle modes are the same as the unconstrained modes a la Hughes[4]. The development here parallels that in the previous subsection on hinges-free modes. Accordingly, introduce the following modal expansion:

$$\underline{V}_0 = \dot{\underline{R}}_0 + \sum \underline{\chi}_{0\alpha}^c\dot{\eta}_\alpha^c(t),\ \sum = \sum_{\alpha=1}^{\infty}$$

$$\underline{\omega}_0 = \dot{\underline{\Theta}}_0 + \sum \underline{\phi}_{0\alpha}^c\dot{\eta}_\alpha^c(t),\ \underline{u}_j = \sum \underline{U}_{j\alpha}^c(\underline{r}_j)\eta_\alpha^c(t) \qquad (31)$$

where the superscript c reminds us that these modal quantities pertain to hinges-locked modes. The quantities $\underline{\chi}_{0\alpha}^c$ and $\underline{\phi}_{0\alpha}^c$ are the translation and rotation of the core body B_0 in α-th mode. Like-

wise, the eigenfunction $\underline{U}^c_{j\alpha}(\underline{r}_j)$ is the deformation of E_j in the α-th mode, analogous to $\underline{U}_{j\nu}(\underline{r}_j)$ in the case of ν-th hinges-free mode, except that now a force is exerted at the hinge 0_j to ascertain that $\underline{U}^c_{j\alpha}(0_j) = \underline{0}$ and $\underline{v}^x\underline{U}^c_{j\alpha}(0_j) = \underline{0}$. The total motion of j-th appendage relative to the B_0-fixed frame in α-th vehicle mode is denoted $\underline{W}^c_{j\alpha}(\underline{r}_j)$ and it equals [cf. Eq. (18)]

$$\underline{W}^c_{j\alpha}(\underline{r}_j) \triangleq \underline{\chi}^c_{0\alpha} - (\underline{b}_j + \underline{C}_{0j}\underline{r}_j)^x \underline{\phi}^c_{0\alpha} + \underline{C}_{0j}\underline{U}^c_{j\alpha}(\underline{r}_j) \tag{32}$$

The α-th mode of the core body, $\underline{W}^c_{0\alpha}(\underline{r}_0)$, on the other hand, will be

$$\underline{W}^c_{0\alpha}(\underline{r}_0) \triangleq \underline{\chi}^c_{0\alpha} - \underline{r}^x_0\underline{\phi}^c_{0\alpha} \tag{33}$$

Thus, like Eq. (20), the α-th mode $\underline{W}^c_\alpha(\underline{r})$ will be $\underline{W}^c_{0\alpha}(\underline{r}_0)$ or $\underline{W}^c_{j\alpha}(\underline{r}_j)$ depending on the domain under consideration. Orthogonality of these modes with the six rigid modes $\underline{1}$ and $-\underline{r}^x$, similar to Eqs. (21.a, 21.b), can be proved easily. To express these conditions in terms of hinges-locked modal momenta coefficients, define [cf. Eq. (22)]:

$$\underline{p}^c_{j\alpha} \triangleq \int_j \underline{U}^c_{j\alpha}(\underline{r}_j)\, dm \qquad \underline{h}^c_{j\alpha} \triangleq \int_j \underline{r}^x_j\underline{U}^c_{j\alpha}(\underline{r}_j)\, dm$$

$$\underline{p}^c_\alpha \triangleq \sum_j \underline{C}_{0j}\underline{p}^c_{j\alpha} \qquad \underline{h}^{0^c}_\alpha \triangleq \sum_j (\underline{b}^x_j\underline{C}_{0j}\underline{p}^c_{j\alpha} + \underline{C}_{0j}\underline{h}^c_{j\alpha}) \tag{34}$$

Then, the above mentioned orthogonality is [cf. Eq. (23)]:

$$m\,\underline{\chi}^c_{0\alpha} - \underline{c}^x\underline{p}^c_{0\alpha} + \underline{p}^c_\alpha = \underline{0}$$

$$\underline{c}^x\underline{\chi}^c_{0\alpha} + \underline{J}\,\underline{\phi}^c_{0\alpha} + \underline{h}^{0^c}_\alpha = \underline{0} \tag{35}$$

The eigenvalue problem obeyed by the α-th hinges-locked mode $\underline{W}^c_{j\alpha}(\underline{r}_j)$ is

$$\underline{L}_j\underline{U}^c_{j\alpha}(\underline{r}_j) = \omega^{c^2}_\alpha\, \underline{C}_{j0}\underline{W}^c_{j\alpha}(\underline{r}_j) \qquad (j=1,\ldots,N) \tag{36}$$

where ω^c_α is the associated hinges-locked frequency. The orthogonality conditions between α-th and β-th modes are

$$\int_V \underline{W}^{c^T}_\alpha \underline{W}^c_\beta\, dm = \sum_j \int_j \underline{U}^{c^T}_{j\alpha}\underline{C}_{j0}\underline{W}^c_{j\beta}(\underline{r}_j)\, dm = \delta_{\alpha\beta}$$

$$\sum_j \int_j \underline{U}^{c^T}_{j\alpha}\underline{U}^c_{j\beta}\, dm - m\underline{\chi}^{c^T}_{0\alpha}\underline{\chi}^c_{0\beta} + (\underline{\chi}^{c^T}_{0\alpha}\underline{c}^x\underline{\phi}^c_{0\beta} - \underline{\phi}^{c^T}_{0\alpha}\underline{c}^x\underline{\chi}^c_{0\beta})$$

$$- \underline{\phi}^{c^T}_{0\alpha}\underline{J}\,\underline{\phi}^c_{0\beta} = \delta_{\alpha\beta}$$

$$\sum_j \int_j \underline{U}^{c^T}_{j\alpha}\underline{L}_j\underline{U}^c_{j\beta}\, dv = \omega^{c^2}_\alpha\,\delta_{\alpha\beta} \tag{37}$$

These are a bit more general than Eqs. (62) of Hughes[4].

With the aid of the expansion (31), momental properties (35), and orthogonality properties (37), the original continuum equations (9) are discretized to

$$m\,\ddot{\underline{R}}_0 - \underline{c}^x\ddot{\underline{\Theta}}_0 - \sum_j \underline{C}_{0j}\underline{c}^x_j\dot{\underline{\Omega}}_j = \underline{f}(t)$$

$$\underline{c}^x\ddot{\underline{R}}_0 + \underline{J}\ddot{\underline{\Theta}}_0 + \sum_j \underline{C}_{0j}\underline{J}_{0j}\dot{\underline{\Omega}}_j = \underline{g}(t)$$

$$\underline{c}^x_j\underline{C}_{j0}\ddot{\underline{R}}_0 + \underline{J}^T_{0j}\underline{C}_{j0}\ddot{\underline{\Theta}}_0 + \underline{J}_j\dot{\underline{\Omega}}_j + \sum_\alpha \underline{h}^{cI}_{j\alpha}\ddot{\eta}^c_\alpha = \underline{g}_{0j} + \underline{g}_j \qquad (j=1,\ldots,N)$$

$$\sum_j (\underline{h}^{cI}_{j\alpha})^T\dot{\underline{\Omega}}_j + \ddot{\eta}^c_\alpha + \omega^{c^2}_\alpha\,\eta^c_\alpha = \underline{\chi}^{c^T}_{\alpha 0}\underline{f} + \underline{\phi}^{c^T}_{\alpha 0}\underline{g} + \gamma^c_\alpha(t) \tag{38}$$

Unlike the hinges-free set of discrete equations (28), the last two equations in (38) involve a new coupling term called "inertial modal angular momentum coefficient" $\underline{h}^{cI}_{j\alpha}$ defined as

$$\underline{h}^{cI}_{j\alpha} \triangleq \int_j \underline{r}^x_j\underline{C}_{j0}\underline{W}^c_{j\alpha}(\underline{r}_j)\, dm =$$

$$\underline{c}^x_j\underline{C}_{j0}\underline{\chi}^c_{0\alpha} + (\underline{J}_j\underline{C}_{j0} - \underline{c}^x_j\underline{C}_{j0}\underline{b}^x_j)\underline{\phi}^c_{\alpha 0} + \int_j \underline{r}^x_j\underline{U}^c_{j\alpha}\, dm \tag{39}$$

which is different from $\underline{h}^c_{j\alpha}$ and $\underline{h}^{0^c}_\alpha$ defined in (34). The disturbance input $\gamma^c_\alpha(t)$ to each α-th mode equals [cf. Eq. (29)]

$$\gamma^c_\alpha(t) \triangleq \sum_j \int_j \underline{U}^{c^T}_{j\alpha}(\underline{r}_j)\underline{\ell}_j(\underline{r}_j,t)\, dA \tag{40}$$

To compact Eqs. (40), introduce

$$\underline{h}^{cI^T}_j \triangleq [\underline{h}^{cI}_{j1}\ \underline{h}^{cI}_{j2}\ \ldots], \qquad \underline{h}^{cI}_A \triangleq [\underline{h}^{cI}_1\ \ldots\ \underline{h}^{cI}_N] \tag{41}$$

Then, recalling pertinent definitions from (13), (15), and (28), Eqs. (38) contract to

$$\underline{M}_{VV}\ddot{\underline{q}}_{VR} + \underline{M}^T_{VA}\dot{\underline{\Omega}}_A = \underline{u}_V(t)$$

$$\underline{M}_{VA}\ddot{\underline{q}}_{VR} + \underline{J}_A\dot{\underline{\Omega}}_A + \underline{h}^{cI^T}_A\ddot{\underline{\eta}}^c_e(t) = \underline{g}_A(t) + \underline{g}_{0A}(t)$$

$$\underline{h}^{cI}_A\dot{\underline{\Omega}}_A + \ddot{\underline{\eta}}^c_e(t) + \underline{\omega}^2_c\underline{\eta}_e(t) = \underline{\chi}^c_0\underline{f} + \underline{\phi}^c_0\underline{g} + \underline{\gamma}_c \tag{42}$$

The vector $\underline{\eta}^c_e(t)$ and $\underline{\gamma}_c(t)$, and the matrices $\underline{\omega}_c, \underline{\chi}^c_0, \underline{\phi}^c_0$ are defined like their hinges-free companions in (28).

IV. MODAL IDENTITIES FOR MULTIBODY ELASTIC SPACECRAFT

Our principal concern is to compare hinges-free and hinges-locked modes for their accuracy in representing articulation motion. To accomplish this aim, an equation will be obtained from each of the above three sets of discrete equations which will be solely in terms of the articulation motion $\dot{\underline{\Omega}}_A$ and stimuli. These three equations will then be compared to yield identities.

First, consider the discrete set (16) based on appendage modes. By matrix manipulations, the following equation governing $\underline{\dot{\Omega}}_A$ can be constructed readily:

$$\left[\underline{1} - \underline{\mathcal{H}}_A^T \left(\underline{\mathcal{U}}_\infty + \underline{\Omega}_C^2/s^2\right)^{-1} \underline{\mathcal{H}}_A \underline{\mathcal{J}}^{-1}\right] \underline{\mathcal{J}}\, \underline{\dot{\Omega}}_A =$$

$$\underline{\mathcal{H}}_A^T \left(\underline{\mathcal{U}}_\infty + \underline{\Omega}_C^2/s^2\right)^{-1} \underline{\mathcal{P}}_A^0\, \underline{M}_{VV}^{-1}\, \underline{u}_V$$

$$-\underline{\mathcal{H}}_A^T \left(\underline{\mathcal{U}}_\infty + \underline{\Omega}_C^2/s^2\right)^{-1} \underline{\gamma}_A^a - \underline{M}_{VA}\, \underline{M}_{VV}^{-1}\, \underline{u}_V + \underline{g}_H \qquad (43)$$

where s is the Laplace variable; theoretically, $\underline{\mathcal{H}}_A$ is an $\infty \times n_a$ matrix, and $\underline{\mathcal{U}}_\infty$ an $\infty \times \infty$ symmetric matrix; $\underline{\mathcal{J}}$ is an $n_a x n_a$ inertia matrix, and $\underline{g}_H$ is the total hinge torque vector:

$$\underline{\mathcal{H}}_A \triangleq -\underline{\mathcal{P}}_A^0\, \underline{M}_{VV}^{-1}\, \underline{M}_{VA}^T + \underline{H}_A, \quad \underline{\mathcal{U}}_\infty \triangleq \underline{1}_\infty - \underline{\mathcal{P}}_A^0 \underline{M}_{VV}^{-1} \underline{\mathcal{P}}_A^{0\,T}$$

$$\underline{\mathcal{J}} \triangleq \underline{J}_A - \underline{M}_{VA}\, \underline{M}_{VV}^{-1}\, \underline{M}_{VA}^T, \quad \underline{g}_H \triangleq \underline{g}_A + \underline{g}_{0A} \qquad (44)$$

In (44), $\underline{1}_\infty$ is $\infty \times \infty$ identity matrix. Thus for an equation of $\underline{\mathcal{J}}\, \underline{\dot{\Omega}}_A$ (s), the coefficient of the hinge torque $\underline{g}_H$ (s) is

$$\left[\underline{1} - \underline{\mathcal{H}}_A^T \left(\underline{\mathcal{U}}_\infty + \underline{\Omega}_C^2/s^2\right)^{-1} \underline{\mathcal{H}}_A\, \underline{\mathcal{J}}^{-1}\right]^{-1} \qquad (45)$$

Anticipating our later needs, now we shall prove that the lim $s\to\infty$ of the matrix $[\bullet]$ in (45) equals

$$\underline{1} - \underline{\mathcal{H}}_A^T\, \underline{\mathcal{U}}_\infty^{-1} \underline{\mathcal{H}}_A\, \underline{\mathcal{J}}^{-1} = \underline{0} \qquad (46)$$

Applying the matrix inversion lemma to $\underline{\mathcal{U}}_\infty$, its inverse is found to be:

$$\underline{\mathcal{U}}_\infty^{-1} = \underline{1}_\infty - \underline{\mathcal{P}}_A^0 \left[\underline{\mathcal{P}}_A^{0\,T} \underline{\mathcal{P}}_A^0 - \underline{M}_{VV}\right]^{-1} \underline{\mathcal{P}}_A^{0\,T} \qquad (47)$$

On the other hand, owing to the identities (D,E,F)" of Hughes[4]

$$\underline{\mathcal{P}}_A^{0\,T} \underline{\mathcal{P}}_A^0 = \begin{bmatrix} m_e \underline{1} & -\underline{c}_e^x \\ \underline{c}_e^x & \underline{J}_e^0 \end{bmatrix} \triangleq \underline{M}_e^0 \qquad (48)$$

Also, by definition of $\underline{M}_{VV}$ in (15), and by virtue of Eq. (1) and Eq. (3)

$$\underline{M}_{VV} = \begin{bmatrix} m_0 \underline{1} & -\underline{c}_0^x \\ \underline{c}_0^x & \underline{J}_0 \end{bmatrix} + \underline{M}_e^0 \triangleq \underline{M}_0 + \underline{M}_e^0 \qquad (49)$$

which reduces $\underline{\mathcal{U}}_\infty^{-1}$ to

$$\underline{\mathcal{U}}_\infty^{-1} = \underline{1}_\infty + \underline{\mathcal{P}}_A^0\, \underline{M}_0^{-1}\, \underline{\mathcal{P}}_A^{0\,T} \qquad (50)$$

A comparison of $\underline{\mathcal{U}}_\infty$ with $\underline{\mathcal{U}}_\infty^{-1}$ amazes. Continuing with the proof nevertheless, call upon the basic identities (D,E,F)" of Hughes[4] to derive the following new identities associated with the articulation degrees of freedom:

$$\underline{H}_A^T\, \underline{H}_A = \underline{J}_A \qquad \underline{H}_A^T\, \underline{P}_A^0 = \underline{C}_A^{0} \qquad \underline{H}_A^T\, \underline{H}_A^0 = \underline{J}_{0A}$$

$$\underline{\mathcal{H}}_A^T\, \underline{\mathcal{H}}_A = \underline{\mathcal{J}} - \underline{M}_{VA} \underline{M}_{VV}^{-1} \underline{M}_0\, \underline{M}_{VV}^{-1}\, \underline{M}_{VA}^T,$$

$$\underline{\mathcal{H}}_A^T\, \underline{\mathcal{P}}_A^0 = \underline{M}_{VA}\, \underline{M}_{VV}^{-1}\, \underline{M}_0 \qquad (I)$$

(New identities derived in this paper will be labeled with Roman numerals as they are cited.) These identities and Eq. (50), in turn, lead to the identity

$$\underline{\mathcal{H}}_A^T\, \underline{\mathcal{U}}_\infty^{-1} \underline{\mathcal{H}}_A = \underline{\mathcal{J}} \qquad (II)$$

which proves Eq. (46)

An equation analogous to Eq. (43) is obtained from the hinges-free discrete set (29). For that, recall the second expansion in (17). Then it can be shown that

$$\underline{\mathcal{J}}\, \underline{\dot{\Omega}}_A = \underline{\mathcal{J}}\, \underline{\phi}_A^T \left(\underline{1}_\infty + \underline{\omega}^2/s^2\right)^{-1} \left(\underline{\chi}_0\, \underline{f} + \underline{\phi}_0\, \underline{g} + \underline{\gamma}\right)$$

$$- \underline{M}_{VA}\, \underline{M}_{VV}^{-1}\, \underline{u}_V(s)$$

$$+ \left[\underline{1} + \underline{\mathcal{J}}\, \underline{\phi}_A^T \left(\underline{1}_\infty + \underline{\omega}^2/s^2\right)^{-1} \underline{\flat}_A\right] \underline{g}_H(s) \qquad (51)$$

The coefficient of the hinge torque $\underline{g}_H$ (s) in Eq. (51) equals the term (45). They both reduce to $\underline{1}$ for the lim $s\to 0$, and for the lim $s\to\infty$ they yield, in view of Eq. (46), the identity

$$\left(\underline{1} + \underline{\mathcal{J}}\, \underline{\phi}_A^T\, \underline{\phi}_A\right)^{-1} = \underline{0} \qquad (III)$$

which proves a fortiori that, since the inertia matrix $\underline{\mathcal{J}}$ is positive definite and $\underline{\phi}_A^T \underline{\phi}_A$ nonnegative definite, the modal coefficients $\underline{\phi}_{jv}$ (j=1,...,N; v=1,...,∞) [Eq. (17)] constitute a nonconverging series.

The hinges-locked discrete set (42) furnishes this equation for $\underline{\Omega}_A$:

$$\left[\underline{1} - \underline{h}_A^{cI\,T} \left(\underline{1} + \underline{\omega}_c^2/s^2\right)^{-1} \underline{h}_A^{cI} \underline{\mathcal{J}}^{-1}\right] \underline{\mathcal{J}}\, \underline{\dot{\Omega}}_A = \underline{g}_H - \underline{M}_{VA}\, \underline{M}_{VV}^{-1}\, \underline{u}_V$$

$$- \underline{h}_A^{cI\,T} \left(\underline{1} + \underline{\omega}_c^2/s^2\right)^{-1} \left(\underline{\chi}_0^c\, \underline{f} + \underline{\phi}_0^c\, \underline{g} + \underline{\gamma}_c\right) \qquad (52)$$

The equality of the coefficient matrices of $\underline{g}_H$(s) in Eq. (51) and Eq. (52) delivers this identity in the s-domain:

$$\left[\underline{1} - \underline{h}_A^{cI\,T} \left(\underline{1} + \underline{\omega}_c^2/s^2\right)^{-1} \underline{h}_A^{cI} \underline{\mathcal{J}}^{-1}\right]^{-1} = \underline{1} +$$

$$\underline{\mathcal{J}}\, \underline{\phi}_A^T \left(\underline{1}_\infty + \underline{\omega}^2/s^2\right)^{-1} \underline{\flat}_A \qquad (IV)$$

For the lim $s\to 0$, the left side of (IV) degenerates to $\underline{1}$ as does its right side. On the other hand, taking its limit $s\to\infty$ and recognizing the identity (III) produce the identity

$$\left[\underline{1} - \underline{h}_A^{cI\,T}\, \underline{h}_A^{cI} \underline{\mathcal{J}}^{-1}\right] = \underline{0} \qquad (V)$$

The identity (IV) can be rearranged such that it reveals poles and zeros of the dynamics. For that, recognize that when $s = \pm j\omega_v$ ($v=1,\ldots,\infty$; $j^2 = -1$) the right side of (IV), which is also the coefficient of $\underline{g}_H$(s) in (51), is unbounded, so $\pm j\omega_v$ are the

poles of the spacecraft. Consequently, for unboundedness to occur, the left side of (IV), expressed in terms of individual hinges-locked modes, yields the identity

$$\det\left[\underline{1} - \sum_{\alpha}\left(1 - \omega_{\alpha}^{c\,2}/\omega_{\nu}^{2}\right)^{-1}\underline{h}_{\alpha}^{cI}\,\underline{h}_{\alpha}^{cI\,T}\,\underline{\mathcal{Q}}^{-1}\right] = 0 \quad \text{(VI)}$$

where $\underline{h}_{\alpha}^{cI\,T}$ is the α-th row of the matrix $\underline{h}_{A}^{cI}$. Similarly, when $s = \pm j\omega_{\alpha}^{c}(\alpha = 1,\ldots)$, the matrix within $[\bullet]$ on the left side of (IV), which is the coefficient of $\underline{\mathcal{Q}}\,\underline{\ddot{\eta}}_{A}$ in (52), is unbounded, which implies that $\pm j\omega_{\alpha}^{c}$ are the zeros of the dynamics. Therefore, to realize unboundedness, the right side of (IV) bears forth

$$\det\left[\underline{1} + \sum_{\mu}\left(1 - \omega_{\mu}^{2}/\omega_{\alpha}^{c\,2}\right)^{-1}\underline{\mathcal{Q}}\,\underline{\phi}_{\mu}\,\underline{\phi}_{\mu}^{T}\right] = 0 \quad \text{(VII)}$$

where $\underline{\phi}_{\mu}^{T}$ is the μ-th row of the matrix $\underline{\phi}_{A}$ [Eq. (28)]. Knowing the poles and zeros, the identity (IV), keeping in mind its lim, has this alternate form [cf. (Y) of Hughes[4]]: $s\to\infty$

$$\left[\underline{1} - \underline{h}_{A}^{cI\,T}\,\underline{h}_{A}^{cI}\,\underline{\mathcal{Q}}^{-1}\right]^{-1}\prod_{\alpha=1}^{n_f}\left(s^2+\omega_{\alpha}^{c\,2}\right)\Bigg/\left[\prod_{\mu=1}^{n_f}\left(s^2+\omega_{\mu}^{2}\right)\right] =$$

$$\left[1 + \underline{\mathcal{Q}}\;\underline{\phi}_{A}^{T}\,\underline{\phi}_{A}\right]\prod_{\alpha=1}^{n_f}\left(s^2+\omega_{\alpha}^{c\,2}\right)\Bigg/\left[\prod_{\mu=1}^{n_f}\left(s^2+\omega_{\mu}^{2}\right)\right] \quad \text{(VIII)}$$

where n_f = total number of retained modes. Because of the identity (V), however, this form seems to be less useful than the form (IV). Following Garg[9], one can examine how far the identities (IV) or (VIII) are satisfied in the s-domain. The identities (VI) and (VII) are useful in several ways; for instance, known hinges-locked parameters can be used to determine hinges-free modal parameters, or vice versa, after Hughes and Garg[10]. Incidentally, the identities (VI) and (VII) are analogous to the identities $(M)_{\theta}$ and (Q) of Hughes[4]. As in Reference 4, under conditions of symmetry, these identities reduce to those concerned with individual articulation degrees of freedom. Owing to symmetry, since different sets of modes will contribute to different articulation degrees of freedom, the set α ($\alpha=1,\ldots,\infty$) may form n_a subsets α_j ($j=1,\ldots,n_a$) and each α_j will span the range $1,\ldots,\infty$; the set μ ($\mu=1,\ldots,\infty$) fragmentates likewise. The identities (VI) and (VII) then simplify to

$$\sum_{\alpha_{\ell}=1}^{\infty}\left(1 - \omega_{\alpha_{\ell}}^{c\,2}/\omega_{\mu_{\ell}}^{2}\right)^{-1}\left[\underline{h}_{\alpha}^{cI}\,\underline{h}_{\alpha}^{CI\,T}\,\underline{\mathcal{Q}}^{-1}\right]_{\ell,k} = \delta_{\ell k} \quad \text{(IX)}$$

$$\sum_{\mu_{\ell}=1}^{\infty}\left(\omega_{\mu_{\ell}}^{2}/\omega_{\alpha_{\ell}}^{c\,2} - 1\right)^{-1}\left[\underline{\mathcal{Q}}\,\underline{\phi}_{\mu-\mu}^{T}\right]_{\ell,k} = \delta_{\ell k}(\ell,k=1,\ldots,n_a) \quad \text{(X)}$$

V. ILLUSTRATION OF MODAL IDENTITIES AND DISCUSSION

The identities will now be illustrated for a four-body deformable spacecraft shown in Fig. 2. It has two flexible solar arrays, E_1 and E_2, each having one articulation degree of freedom about y_1- and y_2-axis, respectively, relative to the core body B_0, and a sensor having two rotational degrees of freedom about x_3- and y_3-axis. These four articulation angles are denoted θ_{1y}, θ_{2y}, θ_{3x}, and θ_{3y}, and the spacecraft thus has ten rigid modes. Hinges-free and hinges-locked vehicle modal data for the spacecraft were obtained by using NASTRAN. From a detailed finite element model having 19,434 degrees of freedom and 3,239 nodes, 63 hinges-free and 67 hinges-locked elastic modes below 25 Hz were computed. Since the vehicle is essentially symmetric (the sensor causes a slight asymmetry), both symmetric and antisymmetric vehicle modes arise in transverse bending and in-plane bending of the arrays, and the vehicle modes are categorized accordingly in Table 1 and Table 2. Fig. 3a confirms the prediction from the identity (III) that the hinges-free modal coefficients, in this case $\phi_{1\mu y}$ ($\mu=1,\ldots,63$) for the y_1-solar array, form a nonconverging series. In Fig. 3a, the largest modal coefficients $\phi_{1\mu y}$ for $\mu=8,11,18,28,\ldots$ correspond to those vehicle modes which predominately entail torsion of the y_1-array about y_1-axis (Table 1). In contrast, those contributing to θ_{3y}, namely, $\phi_{3\mu y}$($\mu=1,\ldots,63$), form essentially a convergent series because the sensor is rigid, and symmetric transverse bending of the arrays (Table 1) or local high-frequency deformation of B_0 at the sensor base produce $\phi_{3\mu y}$ ($\mu=1,\ldots,63$). The hinges-locked coupling coefficients $h_{1\alpha y}^{cI}$ for y_1-array and $h_{3\alpha y}^{cI}$ for θ_{3y} rotation for the modes $\alpha=1,\ldots,67$ are displayed in Fig. 4. Unlike $\phi_{1\mu y}$, $h_{1\alpha y}^{cI}$ forms a converging series.

The identities (III) and (V) are the simplest, for they involve only modal coefficients, no frequencies. The identity (III) is illustrated in Fig. 5. The error indexes e_{kk}^{HF} (k=1, 3) (HF means hinges-free) are the corresponding diagonal elements of the (4x4) matrix $\left[\underline{1} + \underline{\mathcal{Q}}\,\underline{\phi}_{A}^{T}\underline{\phi}_{A}\right]^{-1}$. In contrast to their zero ideal value, the asymptotes

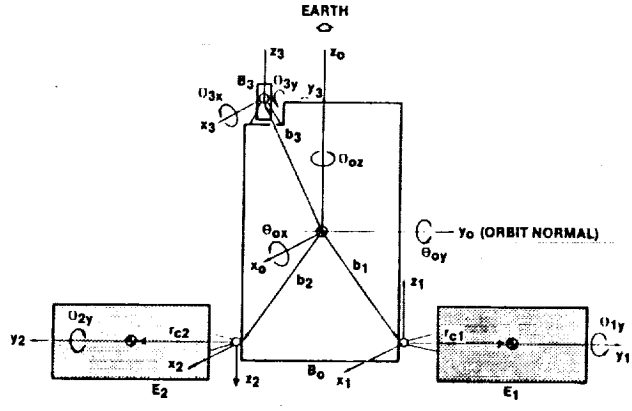

Figure 2. A Four-Body Deformable Spacecraft

Table 1. Hinges-Free Modes

Characteristics of the Mode		Mode No.	Affected Rotational Degrees of Freedom
Transverse bending of arrays and A-frames	Symmetric	1, 5, 9, 13, 15, 21, ...	θ_{oy}, θ_{3y}
	Antisymmetric	2, 6, 10, 14, 16, 22, ...	θ_{oz}
Torsion of arrays and A-frames	Array 1	8, 11, 18, 28, ...	θ_{1y}
	Array 2	7, 12, 19, 29, ...	θ_{2y}
In-plane bending of the A-frames and solar arrays	Symmetric	3, ...	None
	Antisymmetric	4, 17, 20, ...	θ_{ox}, θ_{3x}

Table 2. Hinges-Locked Modes

Characteristics of the Mode		Mode No.	Affected Rotational Degrees of Freedom†
Transverse bending of arrays and A-Frames	Symmetric	1, 2, 6, 8, 12, 16	θ_{oy}
		1, 2, ...	θ_{3y}
	Antisymmetric	3, 9, 13, 17, 20, 27, ...	θ_{oz}
Torsion	Array 1	5, 6, 10, 11, 14, 15, 22, 23, ...	θ_{1y}
In-plane bending of arrays and A-frames	Antisymmetric	7, 18, 21, ...	θ_{ox}
		18, ...	θ_{3y}
Vibrations of the spacecraft		28, 35, 36, 37, 41, 42, 43, 44, 47, 48, 49, 53, ...	θ_{ox}
		28, 36, 37, 41, 42, 43, 44, 45, 47, 48, 49, 53, ...	θ_{oy}
		28, 35, 36, 37, 38, 41, 42, 43, 44, 47, 48, 53, ...	θ_{oz}
†Information about the interaction with θ_{2y} and θ_{3x} not available			

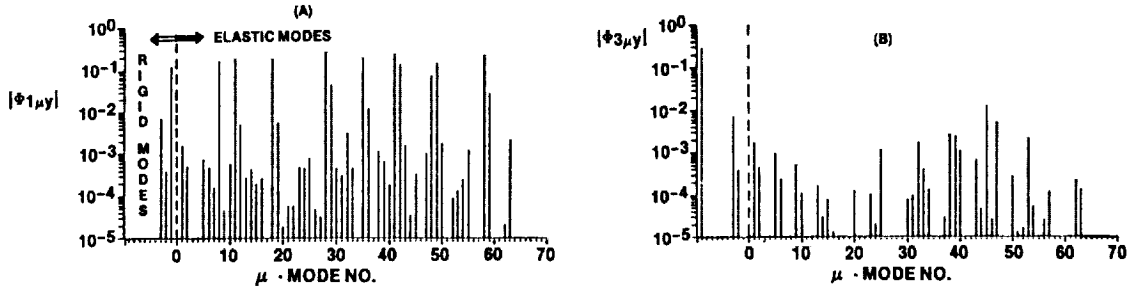

Figure 3. Hinges-Free Modal Coefficients of Articulation Motion of y_1- Solar Array, $|\phi_{1\mu y}|$, and of Sensor B_3, $|\phi_{3\mu y}|$, about y_3-Axis

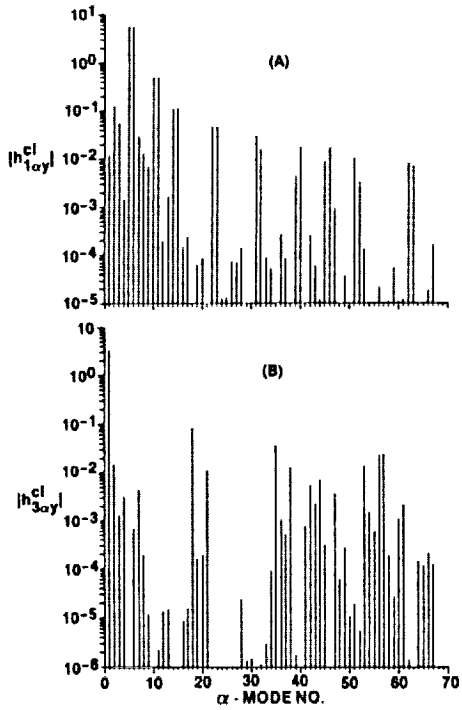

Figure 4. Hinges-Locked Modal Coefficients Associated with the Articulation Motion of y_1-Solar Array, $|h^{cI}_{1\alpha y}|$, and of the Sensor about y_3-Axis, $|h^{cI}_{3\alpha y}|$

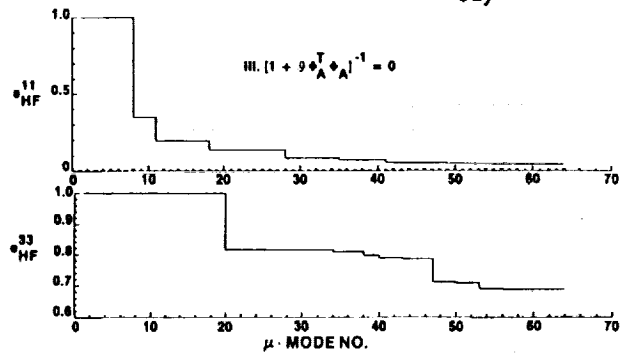

Figure 5. Hinges-Free Identify III: Diminishing of Error Index with Hinges-Free Modes μ

of these indexes are 0.0406 for k=1 (θ_{1y} rotation of the y_1-array) and 0.689 for k=3 (θ_{3x}, the x-rotation of the sensor). The error indexes diminish discretely at appropriate modes as predicted by Table 1. For instance, for θ_{1y}, the error index e^{HF}_{11} diminishes at the torsional modes μ=8,11,18,28,.... The index for the y_2-array motion (k=2) is the same as that for k=1, except that it decreases instead at the adjacent torsional modes μ=7,12,19,29,... (see Table 1). Surprisingly, the asymptote of the error index for θ_{3y} (k=4), not included in Fig. 5, hovers at 0.9976 instead of decreasing to the ideal value zero. Fig. 6 illustrates the hinges-locked identity (V), rearranged as $\underline{h}_A^{cI^T}\underline{h}_A^{cI}\underline{0}^{-1} = \underline{1}$. For discussing this identity and the ones following, define a "completeness index C" which approaches unity for an error-free model [Reference 1]. [The completeness index for Fig. 5 is

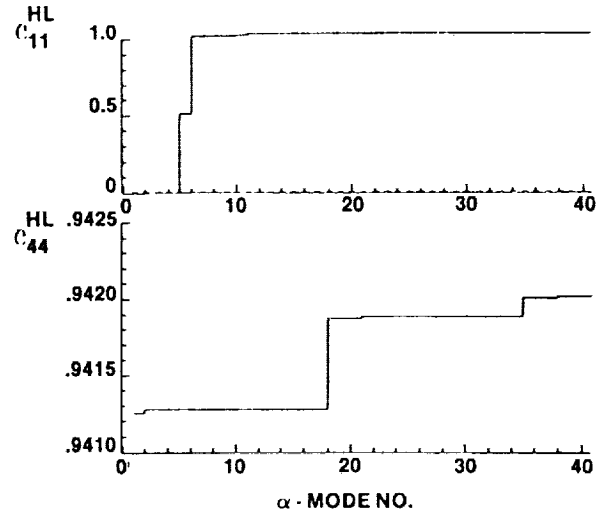

Figure 6. Hinges-Locked Identify V: Growth of Completeness Index with Hinges-Locked Modes α

$(1 - e^{HF}_{kk})$.] The growth of the diagonal elements (1,1) and (4,4) of the matrix $\underline{h}_A^{cI^T}\underline{h}_A^{cI}\underline{0}^{-1}$ are depicted in Fig. 6. Surprisingly, alongside the error index e^{HF}_{11} in Fig. 5a, C^{HL}_{11} (HL means hinges-locked) approaches unity in just two hinges-locked torsional modes, 5 and 6 (Table 2), and its asymptotic value is 1.029. Furthermore, by contrast with the hinges-free completeness index C^{HF}_{44} equal to 0.0024 (that is, the above mentioned error index e^{HF}_{44} of 0.9976), the hinges-locked completeness index C^{HL}_{44} = 0.9421 in Fig. 6b is remarkable; in fact, the first hinges-locked mode, a symmetric transverse bending mode of the arrays (Table 2), contributes a mighty share, 0.9412, to C^{HL}_{44}.

The identities which involve frequencies as well are now illustrated. First, consider the identity (VII) which is summed over all hinges-free modes (μ=1,...,63) for a specific ω^c_α. When ω_μ and ω^c_α are the same to several decimal places, it is difficult to verify this identity in this form. On the other hand, the identity (VIII) indicates that when ω_μ and ω^c_α are truly the same, the corresponding poles and zeros cancel each other without affecting the articulation dynamics. A physical explanation of this is that when hinges-free and hinges-locked frequencies are truly equal, that particular mode does not contribute to the articulation motion, so such a mode may be deleted from the study. In numerical work, however, it is difficult to establish true equality between two real numbers. Besides, as will be seen shortly, for the example in hand, sometimes even though ω_μ and ω^c_α are the same up to three or four decimal places, the minuscule difference between the two is still important for the verification of an identity. Consequently, the following results are obtained without truncating either modal set. Returning to the identity VII, one finds that when $\alpha > 9$, hinges-locked frequencies ω^c_α are so close to a corresponding hinges-free frequency ω_μ that the determinant, instead of being zero, becomes an arbitrarily

large number. Among $\alpha=1,\ldots,9$, the identity (VII) is best satisfied with $\alpha=7$ and next best with $\alpha=2$, for which the determinants are, respectively, -0.00415 and 0.04732 (Table 3). The circumstances which produce these results are revealed by the identity (X). For a given ω_α^c, when all available hinges-free modes are added to calculate the (ℓ,k) element of the left side of (X), it is denoted $C^{HF}_{\ell k,asy}$ where "asy" means asymptotic value. Fig. 7 shows $C^{HF}_{\ell\ell,asy}$ for $\ell=1,3$, and 4. The ideal value of this index is unity; however, when $\omega_{\mu_\ell} \approx \omega^c_{\alpha_\ell}$ for some μ and α, this index assumes an arbitrarily large value, and for plotting purposes, such large numbers are replaced by 2 without altering their signs. In the left side of Fig. 7.a, in the useful range 0 to 1, the maximum value of $C^{HF}_{11,asy}$ concerning the y_1-array rotation, θ_{1y}, is 0.451 for the hinges-locked mode $\alpha=2$-- a symmetric transverse bending mode of the arrays (Table 2). On the other hand, the first torsional hinges-locked mode having significant coupling with the rotation θ_{1y} is $\alpha=5$ (Table 2 and Fig. 4), but $C^{HF}_{11,asy}$ corresponding to $\alpha=5$ is 0.16, less than 0.451 for $\alpha=2$. Although the index $C^{HF}_{11,asy}$ for $\alpha=5$ should be, intuitively, greater than that for $\alpha=2$, this does not happen because the hinges-free frequency ω_1 (0.25724 Hz) is close to ω_2^c (0.25719 Hz). To determine the contribution of the mode $\mu=1$, the growth of C^{HF}_{11} with successive addition of μ to the asymptotic value 0.451 for $\alpha=2$ is shown in the right side of Fig. 7.a. C^{HF}_{11} is found to escalate discretely at $\mu=1,8,11,18,28,29,35,41,42,\ldots$, which, except for $\mu=1$, involve torsion of the array 1 (Table 1). The contribution from the hinges-free mode $\mu=1$, a symmetric transverse bending mode of the arrays (Table 1) like $\alpha=2$ hinges-locked mode, is however, extraordinarily large: 93%. Nevertheless, the bending mode $\mu=1$ is not pertinent to the articulation motion θ_{1y}, so $C^{HF}_{11}=0.451$ for $\alpha=2$ cannot be accepted, and, instead, $C^{HF}_{11}=0.16$ for $\alpha=5$, a torsional mode is accepted. Next consider the sensor motion θ_{3x}. The corresponding index, $C^{HF}_{33,asy}$, shown on the left side of Fig. 7.b, is 1.0059 for $\alpha=7$ (compare with $C^{HF}_{11,asy}$, and recall from Table 3 the value 0.00415 of the identity VII for $\alpha=7$). The growth of C^{HF}_{33} versus μ for $\alpha=7$ is displayed on the right side of Fig. 7.b, where it is observed to become unity at once when $\mu=4$. To understand this, note that both $\mu=4$ and $\alpha=7$ modes involve antisymmetric in-plane bending of the arrays--a motion which induces θ_{3x} (see Table 1 and Table 2), and that $\omega_4=0.59541$ and $\omega_7^c=0.59538$ Hz. When the rotation θ_{3x} of the rigid sensor is locked, the moment of inertia which must be turned by the antisymmetric in-plane bending, is increased, and that lowers the frequency commensurately. The ratio of the moment of inertia of the sensor and of the core body, both about x_0-axis, is 0.0717. The decrement of 3.0E-5 Hz noted above in the frequency ω_4 is mathematically so precise that C^{HF}_{33} becomes unity at once when $\alpha=7$. Moreover, although ω_4 and ω_7^c are the same up to three decimal places, the two modes cannot be truncated from the study of the verification of the identities VII and X. Next, consider θ_{3y} rotation of the sensor--the rotation coupled with the transverse symmetric bending of the arrays (Table 1 and Table 2). The associated index, $C^{HF}_{44,asy}$, versus α is shown in Fig. 7c. In the range 0 to 1, the most it becomes is a startling low value: 0.07836 for $\alpha=2$; for this α, the growth of C^{HF}_{44} with μ indicates that 99.99% contribution arises from the first symmetric transverse bending mode $\mu=1$.

The verification of the identity (IX) for $\ell=k=1$ and 4 is considered in Fig. 8. Since this identity relates to hinges-locked modal parameters, its left side is denoted $C^{HL}_{\ell k}$. Earlier, the identity (V) and Fig. 4 established that the hinges-locked coupling coefficients form a converging series. Therefore, the determinant identity (VI) and $C^{HL}_{\ell k,asy}$ in Fig. 8 do not become arbitrarily large numbers once $\mu \geq 28$. Indeed, only for $\mu=3,4,21,26,27$, is the index $C^{HL}_{\ell k,asy}$ unbounded, by contrast with the hinges-free index $C^{HF}_{11,asy}$ in Fig. 7a which is unbounded for all $\alpha \geq 9$. The index $C^{HL}_{\ell\ell}$ depends on the selected hinges-free frequency ω_μ; for α's having $\omega_\alpha^c > \omega_\mu$, the term $(1-\omega_\alpha^{c\,2}/\omega_\mu^2)$ becomes negative and these particular hinges-locked modes diminish the sum. Focusing first on $C^{HL}_{11,asy}$, surprisingly, it stabilizes early on to 1.05 when $\mu=7$ or 8--the first two hinges-free torsional modes. The ascent of C^{HL}_{11} to 1.05 for $\mu=8$ with hinges-locked modes α (Fig. 8a) indicates significant contributions from $\alpha=5,6,10$, and 11--all torsional modes (Table 2); the contribution from higher torsional modes attenuates rapidly because of the fast convergence of $\underline{h}^{cI}_{1\alpha y}$. As for the rotation θ_{3y}, the maximum value of $C^{HL}_{44,asy}$, displayed in Fig. 8b, in the range 0 to 1 is 0.959 when $\mu=5$--the second hinges-free symmetric transverse bending mode of the arrays (Table 1). The growth pattern of C^{HL}_{44} versus α for $\mu=5$, also shown in Fig. 8b, states that virtually the entire contribution arises from the first hinges-locked mode ($\alpha=1$) involving symmetric transverse bending of the arrays.

VI. SUMMING UP

To draw conclusions about the relative merits of hinges-free and hinges-locked vehicle modes, Table 4 summarizes the completeness indexes for the identities (III), (V), (IX), and (X). Evidently, the hinges-locked indexes are far closer to unity than the hinges-free indexes. The superiority of the hinges-locked vehicle modes to the hinges-free modes is established most persuasively by comparing the indexes for the articulation motion θ_{3y} of the sensor: $C^{HF}_{44,asy}$ are 0.0024 and 0.0784--far remote from unity, whereas $C^{HL}_{44,asy}$ are 0.9421 and 0.9593--almost unity. It must be understood, nevertheless, that the identities (X) and (IX) (or VII and VI)

Table 3. Identity VII: Variation of the Hinges-Free Determinant With Hinges-Locked Modes; Ideal Value = 0

α	1	2	3	4	5	6	7	8	9
VII	0.97105	0.04732	0.27012	0.79457	0.68305	0.68009	-0.00415	0.19551	-0.32426
Minimum value of the determinant among those for α = 10,..., 63, is 74.4, and the maximum value is ∞ when $\omega_\mu = \omega_\alpha$ up to several decimal places									

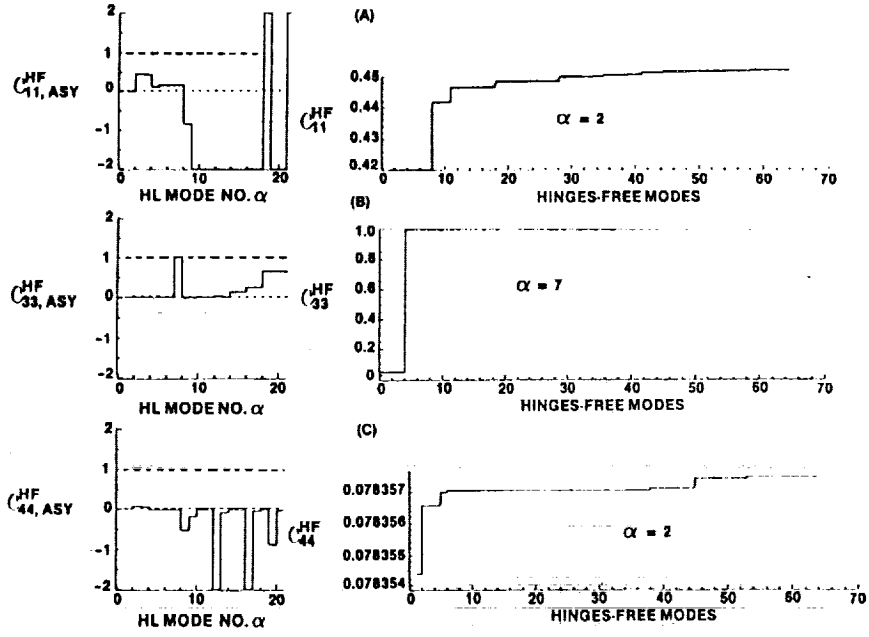

Figure 7. Identity X: Asymptotic Values of the Hinges-Free (HF) Completeness Indexes Versus Hinges-Locked (HL) Mode α, and Growth of this Index Versus Hinges-Free Modes

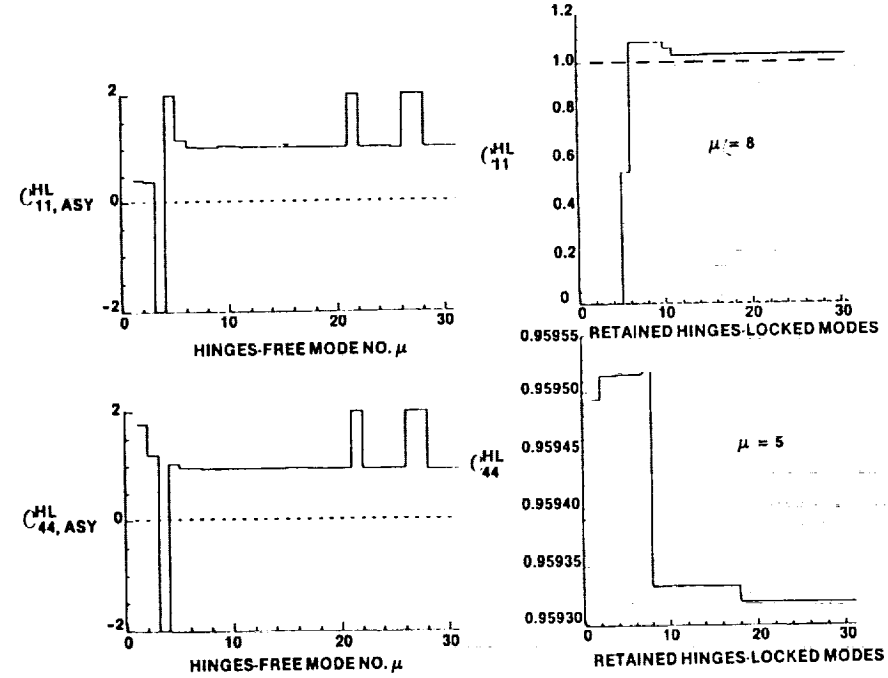

Figure 8. Identity IX: Asymptotic Values of the Hinges-Locked Completeness Indexes Versus Hinges-Free Modes, and Growth of this Index with Hinges-Locked Modes

Table 4. A Summary of the Completeness Indexes for Hinges-Free and Hinges-Locked Vehicle Modes; Ideal Value = 1

Hinges-Free (HF) Indexes	Identity III $1-e^{HF}_{\ell\ell,asy}$	Identity X	Hinges-Locked (HL) Indexes	Identity V	Identity IX	Articulation Motion	Associated Mode of Deformation
$C^{HF}_{11,asy}$	0.9594	0.160	$C^{HL}_{11,asy}$	1.029	1.05	θ_{1y}	Torsion
$C^{HF}_{33,asy}$	0.311	1.0059	$C^{HL}_{33,asy}$	TBD†	TBD†	θ_{3x}	Antisymmetric in-plane bending
$C^{HF}_{44,asy}$	0.0024	0.0784	$C^{HL}_{44,asy}$	0.9421	0.9593	θ_{3y}	Symmetric transverse bending
†to be determined							

represent two different situations: in the former, the hinges-free modes are employed to yield a bounded response at a hinges-locked frequency; and in the latter, the hinges-locked modes are used to elicit an unbounded response at a hinges-free frequency. Therefore, a comparison of the indexes from these identities is slightly inappropriate perhaps; yet the conclusion from Table 2 seems inevitable that the hinges-locked vehicle modes yield a much more accurate model for simulation than the hinges-free vehicle modes do. This is caused by the nonconvergence of the hinges-free modal coefficients in contrast with the rapid convergence of the hinges-locked coupling coefficients--the attributes corroborated by the identities. Besides contrasting one family of modes with the other, the identities are clearly useful in sifting through scores of finite-element generated modes to select a few pertinent modes for an articulation degree of freedom in consideration. An important extension of the preceding work is to devise identities which involve modal coefficients and frequencies of only one family of modes, hinges-free or hinges-locked, not both. Hughes[11] has formulated such identities for an elastic body with no articulated members.

ACKNOWLEDGEMENTS

The numerical results in this paper were obtained by Mr. Thomas C. Witham, Avionics Systems Group. The author thanks him with much pleasure for his painstaking and conscientious efforts.

REFERENCES

1. Hablani, H.B., "Constrained and Unconstrained Modes, Some Modeling Aspects of Flexible Spacecraft," Journal of Guidance and Control, Vol. 5, No. 2, March-April, 1982, pp. 164-173.

2. Hughes, P.C., Dynamics of Flexible Spacecraft, UCLA Lecture Notes (1982).

3. Hablani, H.B., "Hinges-Free and Hinges-Locked Modes of a Deformable Multibody Spacecraft--A Continuum Analysis," AIAA 87-0925 CP, Proceedings of the AIAA Dynamics Specialist Conference, Monterey, California, April 1987, Part 2B, pp. 753-768.

4. Hughes, P.C., "Modal Identities for Elastic Bodies with Application to Vehicle Dynamics and Control," Transactions of ASME, Journal of Applied Mechanics, Vol. 47, March 1980, pp. 177-184.

5. Ho, J.Y.L., "Direct Path Method for Flexible Multibody Spacecraft Dynamics," Journal of Spacecraft and Rockets, Vol. 14, No. 2, February 1977, pp. 102-110.

6. Hughes, P.C., Spacecraft Attitude Dynamics, Section 3.6, John Wiley and Sons, New York, 1986, pp. 70-76.

7. Hughes, P.C., "Dynamics of a Chain of Flexible Bodies," The Journal of the Astronautical Sciences, Vol. 27, No. 4, October-December 1979, pp. 359-380.

8. Singh, R.P., VanderVoort, R.J., and Likins, P.W., "Dynamics of Flexible Bodies in Tree Topology--A Computer-Oriented Approach," AIAA Paper No. 84-1024, pp. 327-337.

9. Garg, S.C., "Frequency-Domain Analysis of Flexible Spacecraft," AIAA Journal of Guidance, Control, and Dynamics, Vol. 5, No. 1, January-February 1982, pp. 54-59.

10. Hughes, P.C., and Garg, S.C., Dynamics of Large Flexible Solar Arrays and Applications to Spacecraft Attitude Control System Design, Institute for Aerospace Studies, University of Toronto, UTIAS Report 179, February 1973.

11. Hughes, P.C., "Space Structure Vibration Modes: How many exist? Which ones are important?," Proceedings of the Workshop on Applications of Distributed System Theory to the Control of Large Space Structures, JPL Publication 83-46, July 1983, pp. 31-47.